ERROR COMPENSATION FOR RADOME MEASUREMENTS

Scott T. McBride
George M. Cawthon

MI Technologies
1125 Satellite Blvd., Suite 100
Suwanee, GA 30024-4629

ABSTRACT

Geometries for measuring radome characteristics can usually be split into two categories. The first category always has the antenna inside the radome pointing along the range axis. The second category has the antenna maintaining a fixed relationship with respect to the radome during each scan of data.

A facility can generally be designed to minimize measurement errors in one of the two geometries, but not both. Many facilities that permit collection of data in both geometries would benefit from the ability to dynamically capture data that lead to measurement errors, then compute and remove the associated errors.

This paper discusses some of the primary error contributors in a dual-geometry radome measurement system, and suggests some mechanisms for capturing and potentially removing those errors.

Keywords: Data acquisition, Measurement diagnostics, Measurement errors, Measurement systems, Radome measurements

1. Introduction

An increasing number of dual-geometry ranges are being built that use coordinated motion [1] to enable the measurement of multiple radome parameters with a minimum of operator intervention. While such a facility offers additional capability and/or throughput, the introduction and control of the extra positioner axes required has an adverse impact on measurement accuracy.

Perhaps the three most common radome parameter measurements are transmission efficiency, boresight shift, and antenna pattern distortion [1, 2, 3, 4]. In the absence of software compensation, required boresight-shift fidelity is ordinarily the most difficult to achieve in a dual-geometry facility. This paper therefore focuses exclusively on boresight shift measurements.

2. Boresight-Shift Geometry Comparison

A dual-geometry radome test system typically includes a multi-axis tracking radar antenna / gimbal mounted on a radome positioner which can rotate the radome in multiple axes relative to the radar antenna. RF beam deflection due to the effects of the signal passing through the radome material is measured by recording the tracking radar antenna motion while mechanically scanning the radome about the antenna. The boresight direction is measured by recording the antenna gimbal angle encoder readouts. The boresight shift is the difference between the boresight direction with and without a radome mounted.

By contrast, a single-geometry radome test system for boresight shift typically has the antenna mounted on a fixed mast, and a down-range X-Y scanner moves to track the boresight null. The fidelity required of the position readings in this geometry is orders of magnitude less than the fidelity required when gimbal angles are used to define the boresight direction. The sources for error are also greatly reduced because the antenna is fixed in place rather than using several stacked axes in simultaneous motion to track the null.

Systems that measure boresight shift generally need to know that quantity very precisely. Therefore, a dual-geometry range will very likely need not only a high-performance gimbal [5] and control system, but also some post-processing of the data with software.

3. Error Sources That Can Be Reduced via Post-Processing

Any system feature that can change the pointing angle of the test antenna or the incident plane wave is a potential error source. Most positioner axes fall into this category. The portion of the axis positioning errors that can be captured by the acquisition system can be compensated by post-processing. The measured positions on all the axes can be combined to form an overall pointing vector. Deflections (horizontal and vertical) can be computed from the ideal pointing vector. This approach accommodates minor differences in fixed-axis positions between the radome-on and radome-off measurements.

Boresight-shift measurements typically involve a servo loop that tracks the boresight null. Servo error in that tracking system leads directly to error in the determination of boresight direction. If that servo error can be captured, and the corresponding position error can be determined, then the position of each tracking axis can be refined by removing the servo error corresponding to that axis. Servo error in a tracking system is typically a high-frequency signal. The time correlation between that signal and the other data must therefore be very good.

The spatial-frequency characteristics of boresight shift vs. scan-axis position have some upper bound for a particular radome. Spatial-frequency content higher than that bound can be filtered out with a digital low-pass filter. Oversampling the data on the scan axis can improve the efficiency of such a filter. Several error sources can contribute to this high-frequency error:

- Vibration in the positioner stack-up
- RF noise
- Latency in servo-error capture
- Servo-error nonlinearity

The accuracy and repeatability of position feedback on each axis are important quantities for measuring boresight shift. The repeatable portion of the inaccuracy could be characterized and corrected. However, because boresight shift is a differential measurement with very slight angular differences, there is little perceived benefit to that approach.

4. Error Sources That Cannot Be Reduced via Post-Processing

There are numerous potential error sources that do not lend themselves to specific correction in software. High-frequency errors induced from any source can be reduced by digital filtering. The emphasis of this paper is on the post-processing of data to remove error, so little detail is provided on errors that cannot be readily corrected.

Latency among capture of pointing angles creates an error in the determination of boresight direction. The magnitude of the error depends on the axis' instantaneous velocity and the amount of latency.

A lack of repeatability in position measurement cannot be compensated in software. This lack of repeatability could result from backlash in the encoder mounting, axis wobble, movement of an axis whose position is not captured, and/or random errors in the encoder itself.

5. Servo-Error Removal

Boresight shift measurements compute the difference in antenna pointing angle with the radome vs. without the radome. Implicit in this measurement is the assumption that the positioning system has aligned the antenna's boresight with the range axis for each measurement. There will, in general, always be non-zero servo error in the tracking subsystem that provides this alignment. The pointing error that corresponds to this servo error directly affects the accuracy of the boresight shift data.

Figure 1 below shows an example of a monopulse error curve. A tracking servo system typically adjusts the antenna position to maintain zero monopulse error. Any servo error in the tracking system is proportional to the vertical axis in Figure 1, which in turn is related to an antenna pointing error on the horizontal axis.

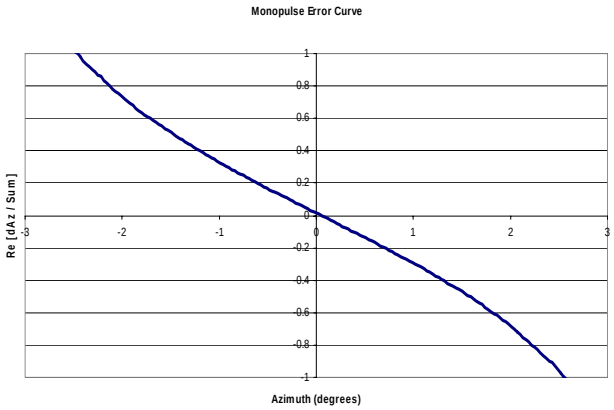

Figure 1 – Monopulse Error Curve

If the tracking servo error is small, the relevant portion of the monopulse error curve in Figure 1 can be approximated as a straight line. Provided the proportionality between the servo-error measurement and the equivalent pointing error is known, the removal of the servo error is straightforward.

Servo error in a tracking system is typically a high-frequency signal. The latency between the servo error and the deflection data must therefore be much less than the period of the oscillation.

The removal of servo error makes the assumption that the slope of the monopulse error curve near boresight does not change significantly when the radome is mounted. To a lesser extent, most tracking systems make a similar assumption. If the slope is expected to change by an unknown amount, the proportionality constant of position error to servo error could be reduced to ensure the data are not overcompensated. The filtering of the data (discussed below) may remove a significant amount of the residual servo error.

6. Compensating Measured Position Data

Boresight shift is a measure of the change in direction of arrival of the primary plane wave. The antenna's global pointing angle while it tracks electrical boresight represents that direction of arrival. This compensation merely removes known errors from that estimate of direction.

This compensation would not be appropriate for facilities that directly measure the antenna's global pointing angle (with an autocollimator, for example). That direct measurement is independent of the positioning errors beneath the antenna.

The basis axes for deflection components should normally be chosen as orthogonal axes in the plane normal to the range axis. For most ranges, horizontal and vertical components are a sensible choice.

The algorithm to use for combining the various measured positions depends upon the stacking of the axes, as well as the desired basis axes for the components of deflection. The equations should be found by generating the 3X3 rotation matrix for each axis, then multiplying them in the proper order.

The algorithm for computing deflection could either perform the above matrix multiplications directly, or could use closed-form equations derived from off-line expansions of that matrix equation. The use of matrix multiplications is straightforward, but inefficient. The closed-form equation approach is described here.

If the deflections are assumed to be small, the equations can be simplified significantly compared to the complete closed-form solution. If we first define deflections as the difference between the actual gimbal angles and the ideal gimbal angles that counter-steer the axes under the gimbal, two rotation stages can be removed from the equations. For example, the angles to counter-steer an az-over-el gimbal on a roll-over-az positioner are

$$Az_{Ant} = Sin^{-1}(Cos(Roll_{Ant})\ Sin(Az_{Lower}))$$

$$El_{Ant} = Sin^{-1}(Sin(Roll_{Ant})\ Sin(Az_{Lower}) / Cos(Az_{Ant}))$$

where $Roll_{Ant}$ and Az_{Lower} are the measured positions on the antenna roll and the lower azimuth axes, and El_{Ant} and Az_{Ant} are the ideal antenna elevation and azimuth angles that would counter-steer the antenna back to the range axis. The locus of points required of such a gimbal to counter-steer a radome azimuth and an antenna roll axis are shown in the figure below. Each trace in the figure represents an azimuth scan of +/-70 degrees with antenna roll fixed at multiples of 15 degrees. The equations above were used to compute the gimbal angles.

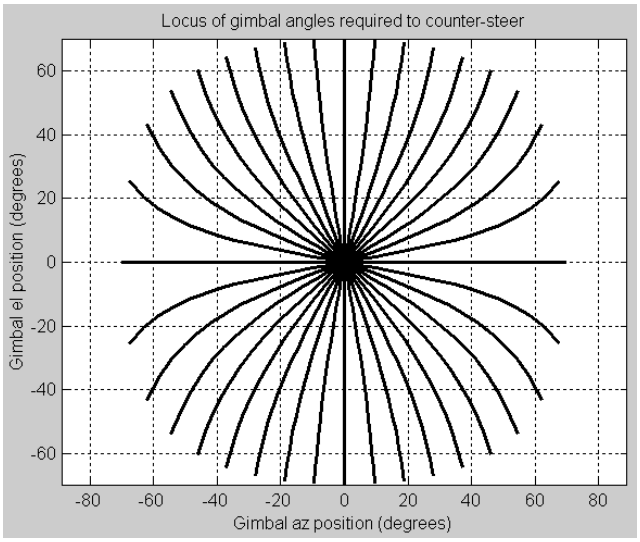

Figure 2 – Locus of gimbal angles required to counter-steer azimuth and roll

Deflections can be computed as the measured gimbal angles minus those ideal angles, and those deflections can then be rotated to the desired basis axes. The deflection for the lower gimbal axis (elevation in this example) must first be multiplied by the cosine of the other measured gimbal axis angle.

Note that in this sample geometry, the rotation of the angular deflections is only equal to the antenna roll angle when azimuth is at zero. At other orientations, the gimbal elevation axis is no longer orthogonal to the range axis and couples into the rotation. An approximate equation for the required rotation ρ (in the sample geometry) is given by:

$$\rho = Sin^{-1}(Cos(Az_{Lower})\ Sin(Roll_{Ant})\ \ Cos(El_{Ant}) + Sin(Az_{Lower})\ Sin(El_{Ant}))$$

where El_{Ant} is the measured gimbal elevation angle. This rotation angle ρ is used as the rotation angle in a standard 2X2 rotation matrix. The vector of two (azimuth and elevation) deflections is multiplied by the rotation matrix, and the result is a vector with the horizontal and vertical components of deflection from the range axis.

This equation for rotation angle ρ assumes that when roll is zero, the gimbal elevation axis of rotation is horizontal. It also assumes that the deflections from ideal are small.

The deflections from ideal gimbal angles should be computed and rotated independently for the radome and free-space data. The beam deflection of the radome is then found as the deflections with the radome minus the corresponding deflections without the radome.

7. Data Filtering

Numerous error contributors, such as vibration and residual servo error, can induce high-frequency error in the beam deflection data. A simple FIR digital low-pass filter can be used [6] (within limits) to reduce the magnitude of those errors. Two filter types, uniform and triangular, are discussed here.

Figure 3 below shows the frequency response of an 11-point uniform filter. The horizontal axis corresponds to the frequency of vibration we are trying to filter out. The vertical axis shows how each frequency of vibration will be attenuated by the filter. The interpretation of this figure requires knowledge of the scan speed and the record increment size, which combine to yield the sample rate in the time domain. If, for example, our scan axis is traveling at 3 degrees/second, and our record increment is 0.1 degrees, then our sample rate is 30 samples per second. The horizontal axis thus ranges from 0 to 15 Hz in this example. If the positioning system has a natural frequency of 9 Hz, this filter in this example would reduce that error by about 90% (output = 0.1 times input). The 11-point filter represents a one-sided filter width of 0.5 degrees.

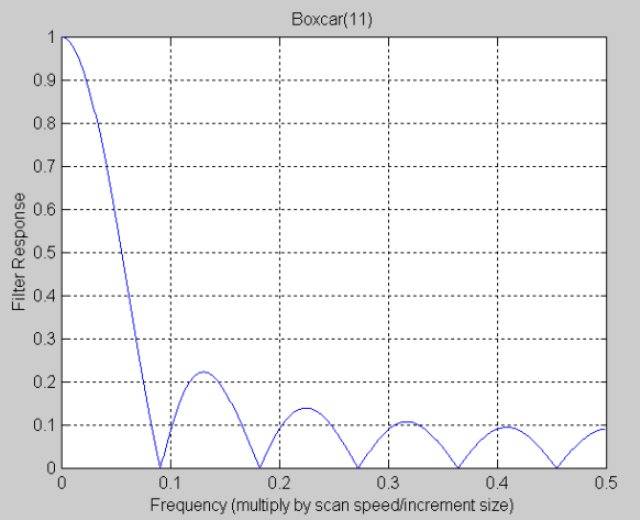

Figure 3 – Frequency response of uniform filter

Figure 4 below shows the frequency response for a triangular filter. This filter has been made a little wider than the first example (15 points vs. 11 points), with the justification that the contribution from the extra samples is small. The extra width was chosen to make the low-frequency response about the same as that of the uniform filter. In the above example with this filter, our 9-Hz vibration is now reduced about 98% (output = 0.02 times input). The 15-point filter represents a one-sided filter width of 0.7 degrees in this example.

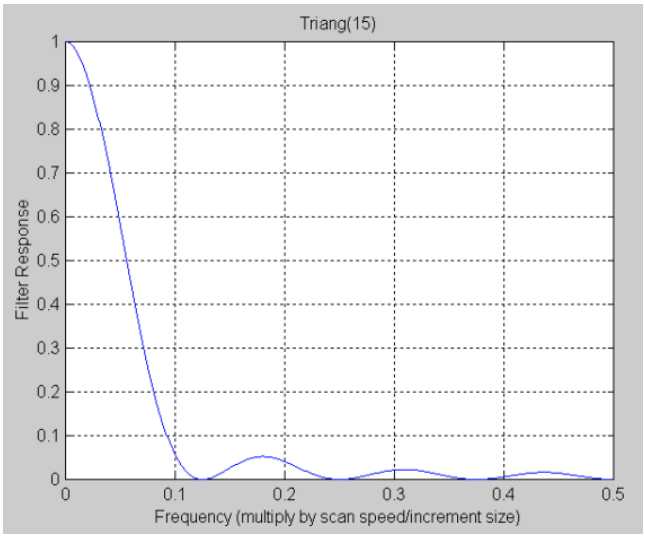

Figure 4 – Frequency response of triangle filter

Figure 5 below shows a random sequence of data synthesized to illustrate the effectiveness of the filtering. (The data were synthesized as a Gaussian white random variable with a mean of 0.5 and a standard deviation of 0.05.) Figure 5 also shows the two example filter windows superimposed, centered on the zero-degree sample. Each filter window is the impulse response of the filter. The filter output is the convolution of the filter input and the filter window. For the uniform window, this is a simple moving average. Any other window represents a weighted moving average.

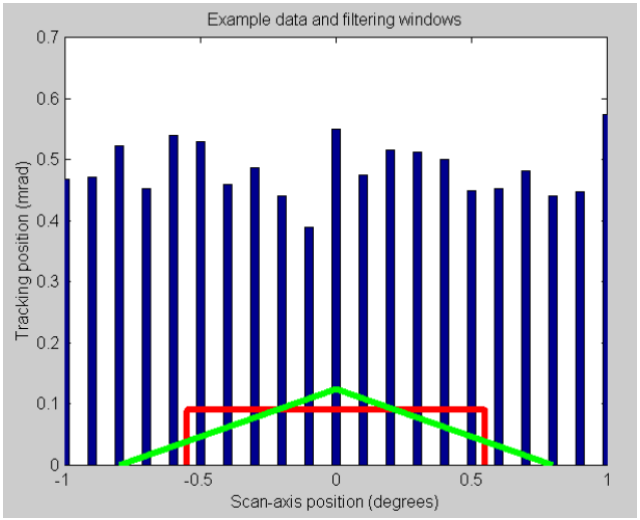

Figure 5 – Synthesized data and example filters

Figure 6 below shows the output of a uniform filter using the data from Figure 5 as input. Note that the data fluctuation is greatly reduced, but that there is still some oscillation.

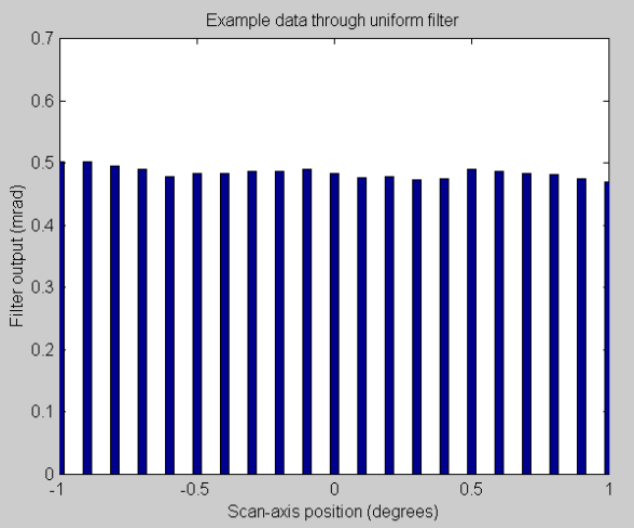

Figure 6 – Sample data after uniform filter

Figure 7 below shows the output of a triangular filter using the data from Figure 5 as input. Note that the data fluctuation is reduced further still, and only low-spatial-frequency content remains.

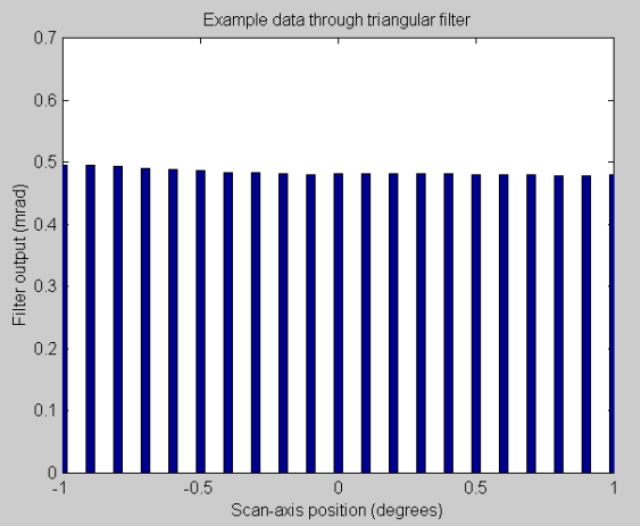

Figure 7 – Sample data after triangle filter

Increasing the width of either filter normally (but not always) results in increasingly smooth output. If, in the extreme case, the uniform filter width were set equal to the range of scan-axis travel, every value of the output of the filter would be the same. While this is certainly a smooth output, it is clearly not the right answer. The best filter will reduce high-frequency vibration noise without attenuating real beam deflection characteristics of the radome.

Reducing the size of the record increment is another way to increase the effectiveness of the filter. The one-sided uniform filter width could be set just under the original record increment, and there will be no artificial correlation among the data samples originally desired. A wider filter can be used if a small radome defect results in deflection over a larger angular range.

8. Implementation

MI Technologies has a radome analysis software package, the MI-3047. Included in the MI-3047 is an application called BDEConversion, which provides optional processing stages for servo-error correction, global pointing angle determination, and spatial filtering.

MI Technologies also has available a Monopulse Tracking Subsystem for use with the MI-2097 data acquisition system. This combination of hardware and software works with the MI-2097 to permit monopulse null tracking, as well as very tight correlation of up to five axes of position plus two channels of tracking servo error.

9. System Design Considerations

In the absence of the software compensation described herein, acceptable boresight-shift measurement fidelity is often the most difficult to achieve in a dual-geometry facility. The use of software compensation permits some relaxation of what can be onerous accuracy, positioning repeatability, and stiffness requirements on each of the axes involved.

Software compensation cannot, of course, overcome the full range of potential problems in a tracking system. The system must support stable tracking in order to acquire the data in the first place. This implies requirements on structural stiffness, motion smoothness, backlash, and RF noise levels.

Compensation using measured positions presumes that those measurements are accurate and/or repeatable. The overall encoder readout accuracy is highly dependent on mounting concentricity of the scale and reading head. This also depends on the encoder / gimbal bearing radial run-out. Bearing run-out and encoder alignment can also be affected by the gimbal's load; thus bearing stiffness is also very important. If we assume that the mechanical load does not change during a scan, a large part of the concentricity error can be corrected. However, a small residual random error will remain that affects beam deflection measurement repeatability. This random component should be less than a fourth of the overall encoder readout accuracy.

Radome scan axis gearing and bearing mechanical noise tend to excite resonant frequencies of the overall radome and radar gimbal structure. The resulting vibrations

introduce false RF beam deflections in the measured data. While these effects can be filtered out of the data via post-processing, it is important that they be minimized with prudent positioner and foundation design.

The use of filtering to remove vibrations presumes that the natural frequencies being filtered are higher than the spatial frequencies expected in the deflection data. The conversion between frequency of vibration and spatial frequency depends upon the scan rate and the size of the record increment. It is best if the lowest natural frequency is between 1/3 and 2/3 the sampling rate (scan speed / increment size). (Due to aliasing, a natural frequency in the range 4/3 to 5/3 or 7/3 to 8/3 of the sample rate would be equally suitable.)

Axis wobble due to bearing axial or radial run out tends to include both bias and random components. The radome pointing position error due to the random component, caused by the shifting of the rollers or balls along the bearing races, cannot be corrected and thus the design must minimize this error.

Whether or not software compensation is incorporated, the capture of the several positions that define beam deflection in a dual-geometry facility must be tightly correlated to each other in order to represent the antenna's pointing angle. If one or more axes are in motion, this implies a maximum latency among the measurements based on the scan speed.

The order in which the various software corrections are applied can be important. The servo-error removal should normally be done as the first stage of processing, since the servo error corresponds to the tracking axes regardless of any positioner error beneath them. The rotation of positioner angles to deflections from the range axis should be done between servo-error removal and filtering. The filtering should normally be done last.

If either the deflection data or servo-error data are filtered prior to the servo-error removal, the other quantity should be filtered in the same way as the pre-filtered data before being subtracted. If an analog filter is used to do that filtering, it will be non-trivial to devise an equivalent digital filter. Special care will be needed to ensure the proper phase lag in the digital filter to maintain time correlation.

The filtering is best performed after a conversion to deflection from the range axis. The gimbal angles, in general, have a non-zero and non-constant slope as they counter-steer roll and/or azimuth angles, as shown in Figure 2. Filtering of such a signal without noise will distort the signal, particularly at the ends of each scan. If the filtered angles were then rotated to deflections from the range axis, error could be introduced. If the filtered gimbal angles are merely compared with and without the radome, however, the result will be identical (due to linearity) to subtracting and then filtering.

If the measurement system is also used to acquire transmission-efficiency (TXE) data, and no software compensation is identified as valid for TXE, then the needs of the TXE data will likely become the driver for the positioning-system requirements.

10. References

[1] McBride, S., Langman, E., Baggett, M., "Applications for Coordinated Motion in Radome Testing", *Proc. of 24th Annual Meeting of the Antenna Measurement Techniques Association (AMTA '02)*, Cleveland, OH, pp. 471-476, November, 2002.

[2] ANSI/IEEE Std 149-1979, *IEEE Standard Test Procedures for Antennas*, pp. 116-119, August, 1980.

[3] RTCA Std DO-213, Minimum Operational Performance Standards for Nose-Mounted Radomes, January, 1993. (Copies of this standard available from RTCA, Inc., 1140 Connecticut Ave NW, Suite 1020, Washington D.C. 20036)

[4] Hollis, J.S., Lyon, T.J., and Clayton, L., eds., Microwave Antenna Measurements, Scientific-Atlanta, Inc., Atlanta, GA, 1985.

[5] Hudgens, J.M, Cawthon, G.M., "Extreme Accuracy Tracking Gimbal for Radome Measurements", *Proc. of 25th Annual Meeting of the Antenna Measurement Techniques Association (AMTA '02)*, Cleveland, OH, pp. 291-295, October, 2003.

[6] Harris, F.J., "On the Use of Windows for Harmonic Analysis with the Discrete Fourier Transform", *Proc. of the IEEE*, Vol. 66, No. 1, pp. 51-83, January, 1978.